Novel experimental procedure and determination of full displacement fields of delaminating composite layer interfaces for evaluation of the mode II cohesive law

Gergely Czél[1,2*], Meisam Jalalvand[1], Michael R. Wisnom[1], Luis P. Canal[3], Carlos D. González[4,5], Javier LLorca[4,5]

[1]Advanced Composites Centre for Innovation and Science, University of Bristol, Queen's Building, BS8 1TR, Bristol, United Kingdom
[2]MTA–BME Research Group for Composite Science and Technology, Budapest University of Technology and Economics, Műegyetem rkp. 3., H-1111 Budapest, Hungary
[3]Laboratory for Polymer and Composite Technology (LTC), Ecole Polytechnique Fédérale de Lausanne (EPFL), Station 12, CH-1015 Lausanne, Switzerland
[4] IMDEA Materials Institute, C/ Eric Kandel 2, 28906, Getafe, Madrid, Spain
[5]Department of Materials Science, Polytechnic University of Madrid, E. T. S. de Ingenieros de Caminos. 28040 - Madrid, Spain
* corresponding author, e-mail: G.Czel@bristol.ac.uk, Tel.: +44 (0) 117 33 15311, Fax: +44 (0) 117 95 45360

Abstract

A novel mode II fracture test setup based on a simple tensile loading scenario with a discontinuous ply specimen is proposed in the paper as the first step towards determination of the cohesive law of composite layer interfaces. Key outputs of the procedure are the full displacement fields obtained by correlation of high resolution SEM images taken during in-situ tensile tests. Analysis of the full displacement fields at subsequent stress levels allow for unique analysis of the damage zone and direct determination of the displacement jumps across the interface. The next

phase of the work is the evaluation of the shear stresses at the interface necessary to determine the

cohesive law.

Keywords:

1. Composites; 2. Cohesive zone modelling; 3. Delamination; In-situ SEM testing

Nomenclature

3PB	three point bending
COD	crack opening displacements
DCB	double cantilever beam
DIC	digital image correlation
EB	electron beam
ENF	end notched flexure
LVDT	linear variable differential transformers
MMB	mixed mode bending
SEM	scanning electron microscope
UD	unidirectional
VCCT	virtual crack closure technique

1. Introduction

Cohesive crack models are one of the classical approaches for predicting and modelling delamination in layered structures such as adhesively bonded joints [1]-[4] and composite laminates [5]-[18]. The modelling technique was initially developed and implemented in FE codes for isotropic materials such as concrete and metals [19]-[22], but spread quickly to composites. The main advantage of this approach over alternative analysis techniques e.g. the virtual crack closure technique (VCCT) is that it includes a nonlinear constitutive material model (cohesive law) that combines crack initiation [23] and propagation [24] criteria and as a result, it can be applied for problems with a variety of loading modes. Cohesive interface elements normally have zero thickness and the interlaminar stress components are coupled to the displacement discontinuities (jumps) across the faces of the deformed element through the cohesive law. Different types of cohesive laws with different shapes e.g. bilinear [10], parabolic [25], exponential [26], trapezoidal [27] etc. were proposed for different materials and validated against experiments. The structures' modelled responses were mostly in good agreement with the test results, and it seems that cohesive laws with different shapes can give similar structural response [25],[28] especially if the crack is much longer than the damage process zone. Most of the modellers therefore use the simplest bilinear shape for the cohesive law and pay attention only to the interfacial shear strength and the fracture toughness. Although, it has been shown that in some problems, the shape of the cohesive law can affect the structural response significantly [29]-[31], the actual shape for composite layer interfaces was not

investigated extensively to date due to difficulties in measuring the very small displacements around the crack tip.

Some researchers studied the cohesive law experimentally with less assumptions. This section aims at giving a short overview of the most important test configurations applied. Sorensen et. al. [32],[33] investigated the effect of fibre-bridging during mixed mode delamination propagation. They derived mixed mode cohesive laws from J-integral values experimentally measured on special specimens. Their experimental setup consists of a cantilever beam (supported with rollers against rotation) incorporating an interlaminar notch at one end, where both layers are loaded with pure but different bending moments. The displacements at the initial notch tip were measured with linear variable differential transformers (LVDT). This complicated but mechanically sound setup is activated by a cable and several rollers. De Moura et al [34] proposed a method for determination of cohesive laws of adhesives experimentally using simple double cantilever beam (DCB) specimens but it can only be applied for mode I loading. The crack opening displacements (COD) were monitored with optical sensors. Fernandes et al [35] used end notched flexure (ENF) specimens under three point bending to determine the mode II cohesive laws of composite bonded joints. The applied external load and displacement were measured and the J-integral was worked out. Then, the cohesive law was obtained based on derivation of the variation of J-integral versus the measured displacement jump at the crack tip. The displacements of the initial crack tip were monitored with a digital image correlation (DIC) system. Dourado et al [36] also executed ENF tests on carbon/epoxy composite samples and determined the mode II cohesive law of the interface inversely by fitting FE data (generated with different piecewise linear cohesive law parameters) to their test graphs. Cui et al [37] applied the advanced but complicated mixed mode bending (MMB) test alignment to evaluate the mixed mode constitutive laws of a 280 μm thick epoxy adhesive layer between woven carbon/epoxy composite plates. The constitutive laws were calculated using a J-integral approach, and DIC

monitoring of the crack opening displacements at the initial position of the pre-crack in the specimen.

The short review of the literature shows that no simple test setup was applied for determination of mode II cohesive laws, and the deformations of the damage process zone were not analysed in detail. Although DIC has been applied in some of the most recent studies [35],[37], this was only on the macroscopic scale to record displacements at the initial crack tip and therefore the full displacement fields of the interfaces were not reported. Most of the previous papers presented investigations of ductile adhesives using a J-integral approach. The stress components were worked out based on estimated or measured displacements at one point close to the initial tip of the crack and the estimated J-integrals.

Micro-scale optical analysis of damage in composites became available recently due to developments of suitable in-situ test apparatuses for simple loading scenarios such as tension, compression and bending. Although in-situ testing was first adapted for the assessment of transverse cracking of unidirectional composite layers [38]-[41], this technique offers scope for an in-depth analysis of mode II damage process zones as well. Gonzalez and LLorca [38] investigated the damage mechanisms in a transversely compressed unidirectional (UD) composite in-situ in a scanning electron microscope (SEM) and identified the key parameters for failure modelling. Canal et al [39] analysed the progression of a tensile transverse crack in a three point bending (3PB) UD composite specimen by executing the tests in-situ in a SEM. Test results were correlated with the outcomes of an embedded cell modelling study and showed good agreement. Canal et al [40] successfully applied DIC on single SEM images in another study to analyse the micro-scale deformations during transverse compression cracking of a UD composite specimen.

The idea behind the present research based on the indications of the literature survey is the following: High resolution micrographs of delaminating composite layer interfaces can be obtained

in-situ in a SEM if a simple loading scenario is found. The SEM images of the deformed specimen can be post-processed with DIC to establish the full displacement fields, which can be used in the next phase for calculating the mode II cohesive law of the interface.

The wider scope of the research is to investigate the delamination initiation and propagation phenomena in detail and propose a procedure by which, the displacement field of adjacent layers of a composite plate made with a brittle epoxy matrix with a very thin interfacial layer can be captured at subsequent stress levels. The displacement fields can then be used for analysis of the displacement jumps as well as the traction (i.e. shear stress) across the interface and finally to evaluate the mode II cohesive law. This methodology provides a deep insight into the deformations of a mode II damage process zone and valuable information such as variation of displacement jump values all along the interface. A novel aspect of the proposed approach is that the tractions and the displacement jumps can be evaluated independently and more directly from the same high resolution displacement field than with other reported techniques.

The overall research aims at exploring the actual shape of the mode II cohesive law of composite layer interfaces. The specific aim of this paper is to present the first step towards the overall goal by the development of a novel experimental procedure to obtain the full displacement field of delaminating interfaces. The approach is to capture the displacements directly on the surface of a progressively delaminating UD composite specimen in a simple loading scenario and analyse the deformations on the micro-scale.

2. Experimental

This section gives a detailed description of the development of a novel test setup and design of matching specimen geometry, which is suitable for in-depth analysis of the deformations around a mode II interlaminar crack in a UD composite. The chosen mechanical testing, image acquisition, post-processing and correlation procedures are discussed as well.

2.1. Development of the novel experimental setup

In order to study the longitudinal displacement field of delaminating composite layers under load with high spatial resolution, the following conditions are necessary: (i) A digital image acquisition device with appropriate magnification and resolution to provide high quality images for deformation analysis (ii) A simple loading device, which can be suitably positioned for image acquisition (iii) The mode II crack propagation during the mechanical test must be stable and allow time for image acquisition at subsequent load steps (iv) The specimen surface of interest showing interlaminar damage and crack propagation must be visible through the imaging system, (v) The observed specimen surface must have features suitable for tracking by an image correlation software, to allow post-processing.

All these requirements can be fulfilled and the displacements of delaminating composite layer interfaces can be captured if a simple tensile test is executed in-situ in the vacuum chamber of a SEM on a specially designed UD composite specimen showing stable mode II crack propagation due to the presence of well positioned ply cuts (see Figure 1.a). The SEM images can be processed with DIC to generate the full displacement field of the delaminating layers (see section 2.8 for more details). The SEM is more suitable than an optical microscope for image acquisition, because it has higher resolution and is able to tolerate small misalignment of the surface of interest. The SEM utilised for the experiments is a Zeiss EVO MA 15 with a relatively large (365 mm (Ø) x 275 mm length) cylindrical vacuum chamber which is able to accommodate a wide range of mechanical testing modules. The simple tensile test was preferred over more complicated bending-based techniques, because it requires less space and it is free of large displacements, therefore more suitable for in-situ SEM testing.

2.2. Specimen design

UD tensile specimens made with cut central plies have been studied experimentally and numerically by Cui et al. [42] to analyse delamination, a key failure mode in layered composites. It was shown that when the specimen is under tension, the interlaminar normal stresses are small, compressive and restricted to the vicinity of the initial cut. Jalalvand et al [43] analysed a similar problem and reported, that the required stress for driving delamination is independent of the interlaminar crack length. The mentioned analysis results indicate that the cut central layer UD specimen design allows for unique interlaminar fracture conditions very close to pure mode II. The discontinuous central layer UD specimens with continuous outer layers which can take the full load after delamination initiation furthermore assures stable propagation of mode II interlaminar cracks, allowing for image acquisition. Similar cut central layer but glass/carbon interlayer hybrid specimens, which show stable central layer pull-out, were used earlier by Czél et al [44] to study the mode II fracture toughness of hybrid composite interfaces. This layer-by-layer hybrid specimen type with a cut central carbon/epoxy and continuous outer glass/epoxy layers was a good starting point for the development of similar architecture but different size specimens suitable for in-situ testing in a SEM chamber. In order to make the delamination of the specimen visible, the 1 mm thick cross-ply glass/epoxy end tabs had to be bonded on the surfaces showing the glass and carbon layers (edges of a specimen cut from a laminated plate). This was necessary because the in-situ tensile module can accommodate specimens only one way round. The specimens were made by curing a 1.5 mm thick laminated hybrid composite plate in an autoclave, and cutting it up into 1.5 mm wide sticks with a diamond wheel to give them 1.5x1.5 mm square nominal cross sections. The end-tabs were bonded on the cut edges of the sticks to let the interesting surfaces, showing the three layer hybrid structure with a cut in the centre of the carbon layer, face towards the electron beam (EB) source when mounted in the SEM tensile module. A schematic of the specimen design and a photograph is shown

in Figure 1. The specimen length was also reduced to make the specimens fit in the available in-situ tensile module.
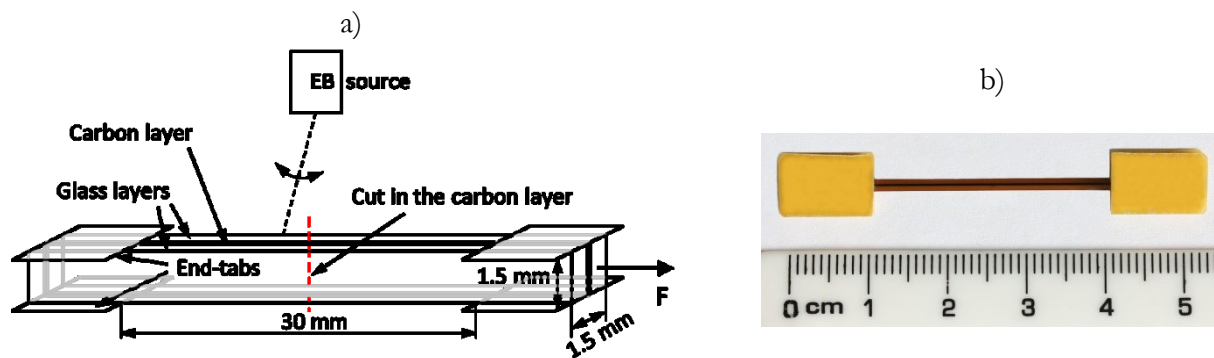

Figure 1. a) Schematic and b) photo of the specimen type developed for in-situ SEM tensile tests

After the geometric design, preliminary tests were executed to confirm that the layers of the specimens delaminate stably. Figure 2. shows the stress-strain graphs of various specimen types with different glass/carbon ratios (controlled by the number of carbon plies in the lay-up sequence) tested in a Shimadzu AGS-X type electro-mechanic test machine with a 10 kN load cell at 2 mm/min crosshead speed. Properties of the constituent materials can be found in tables 1. and 2. Please note that the carbon prepreg was a special thin type only 0.03 mm thick, compared with the standard 0.14 mm glass prepreg. The extensions were measured over a 25 mm gauge length with an Imetrum video gauge system.
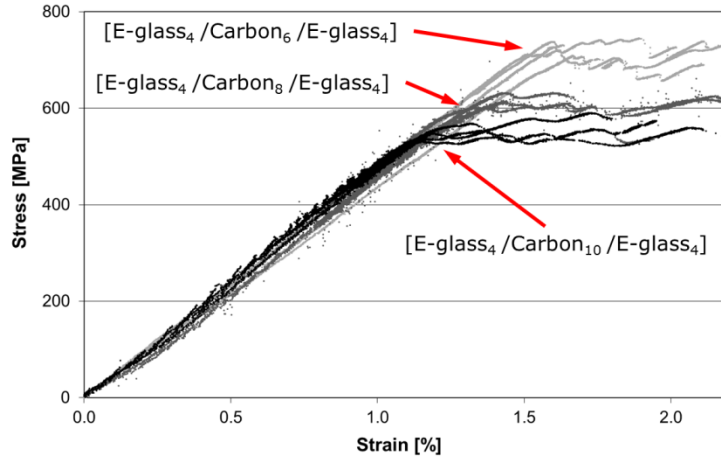
Figure 2. Tensile test results summary of 1.5x1.5x30 mm³ nominal size UD glass/carbon- epoxy hybrid specimens with a single cut through the central carbon/epoxy layer

All specimens failed in a favourable way, showing progressive failure at the layer interfaces in the form of stable mode II crack propagation. Earlier delamination initiation strains were observed in specimen types with thicker carbon layers because of their higher mode II energy release rates. The crack propagation plateaus of the thickest specimen configuration with 10 plies of carbon were the most stable, suitable for step-by-step acquisition of the displacement field on the edge of the specimen at subsequent load levels. Therefore this specimen configuration with stacking sequence: [E-glass$_4$ /Carbon$_{10}$ /E-glass$_4$] was selected for the in-situ SEM tests.

2.3. Specimen surface preparation

The cut surfaces of the fabricated specimens were not suitable for high quality SEM imaging and did not have suitable texture for DIC and therefore it was necessary to prepare them. The cured composite plates were cut roughly to the specimen size and one edge of each specimen (i.e. one showing the layered hybrid structure) was wet polished using SiC papers down to P2500 grit size followed by diamond suspension polishing down to 1 μm particle size. A speckle pattern was then created on this surface by depositing submicron alumina particles from a suspension containing 1 mass % Al$_2$O$_3$ in propanol. The agglomerated particles were broken up to smaller pieces in an ultrasound bath before application. The particle coated specimen surfaces were sputtered with gold

to avoid charging due to the electron beam in the SEM chamber. Figure 3. shows a typical micrograph of the particle coated surface of the specimens.
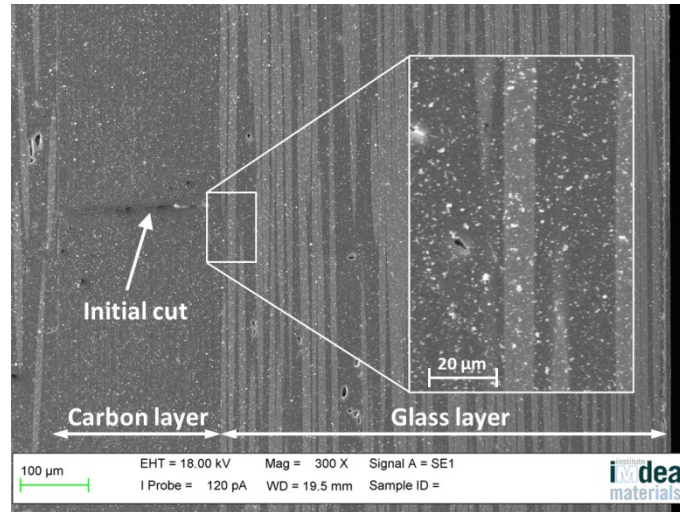

Figure 3. Typical scanning electron micrograph showing the alumina particle coated surface of the tensile specimens (Light grey bands are individual glass fibres, bright white spots are the alumina particles.)

2.4. Materials

The materials considered for specimen design, and applied for the experiments were selected to be consistent with the authors' previous studies [43]-[46] and because of high mismatch between the stiffness of the carbon and glass layers, which is useful for stabilising the stress in the plateau region of the stress-strain curve. Furthermore glass/carbon hybrid composites are widespread and their delamination behaviour is of high interest to the scientific community. In particular they have been used in our recent work on pseudo-ductile composites which produce gradual failure by stable fragmentation of the thin carbon plies [45]. Please note that this study primarily focuses on the damage and fracture of the interface between unidirectional composite layers, the specific materials were selected because of their suitability to approve the novel experimental concept. Therefore the test setup may be suitable for other material combinations as well if stable delamination is assured. The materials applied in this study were E-glass/913 epoxy prepreg supplied by Hexcel, and Sky Flex

11

USN 020A carbon/epoxy prepregs from SK Chemicals made with high strength Pyrofil TR30 carbon fibres produced by Mitsubishi Rayon. Both resin systems in the hybrid laminates were 120°C cure epoxies, which were found to be compatible, although no details were provided by the suppliers on the chemical formulation of the resins. Good integrity of the hybrid laminates was confirmed during composite processing, specimen fabrication and testing and no phase separation was observed on micrographs. Material properties of the applied fibres and prepreg systems can be found in tables 1. and 2.

Table 1. Fibre properties of the applied UD prepregs (based on manufacturer's data)

Fibre type	Manufacturer	Elastic modulus	Strain to failure	Tensile strength	Density
		[GPa]	[%]	[GPa]	[g/cm³]
Pyrofil TR30 carbon	Mitsubishi Rayon	234	1.9	4.4	1.79
EC9 756 P109 E-glass	Owens Corning	72	4.5	3.5	2.56

Table 2. Cured ply properties of the applied UD prepregs

Prepreg material	Property	Fibre mass per unit area	Cured ply thickness	Fibre volume fraction	Initial elastic modulus	Strain to failure	Interlaminar shear strength
	Unit	[g/m²]	[mm]	[%]	[GPa]	[%]	[MPa]
TR30 Carbon/ epoxy	Average	21.2[45]	0.029[45]	41[45]	101.7[47]	1.9[45]	-
	CoVª [%]	4.0[45]	-	-	2.75[47]	6.76[45]	-
E-glass/ epoxy	Average	192ᵇ	0.140[45]	54[45]	40ᵇ	3.7[48]/2.8[45]c	100[49]
	CoV [%]	-	-	-	-	-	-

ªCoefficient of variation
ᵇBased on manufacturer's data
cMeasured on different specimen types in tension

2.5. In-situ tensile testing procedure

A Kammrath&Weiss tensile-compression module equipped with a 10 kN load cell was applied for the in-situ tensile tests at crosshead speeds from 0.05 to 0.5 mm/min (higher speeds in the initial elastic regime, lower speeds towards interlaminar crack initiation and propagation). The module

shown in Figure 4. was designed to move both grips aside with the same speed to keep the centre of

the specimen in the same position during the tensile test, making the image acquisition easier.
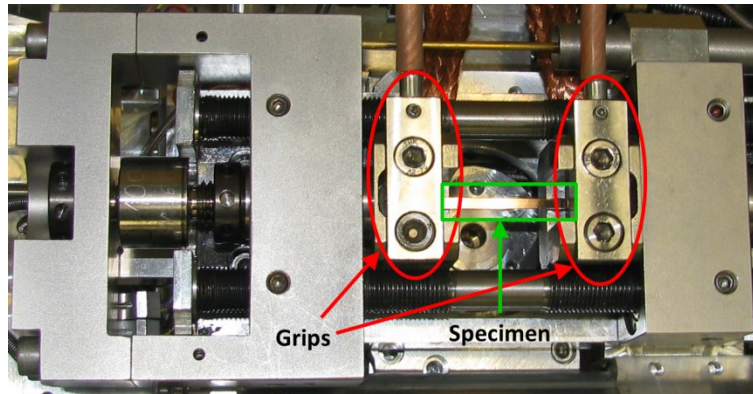

Figure 4. Photograph of the Kammrath&Weiss tensile module for in-situ testing in SEM (the separation between the grips is ~30 mm)

Figure 5. shows typical load-time and load-extension graphs of the in-situ tensile tests. Significant

stress relaxation was observed after the crosshead was stopped for image acquisition and therefore

sufficient relaxation time (~10 min) was left at each load step before scanning the specimen surface

in a quasi-steady state (see Figure 5a). The load-steps were designed to highlight the fracture

behaviour around the expected plateau, so early steps were set to be bigger and then they were
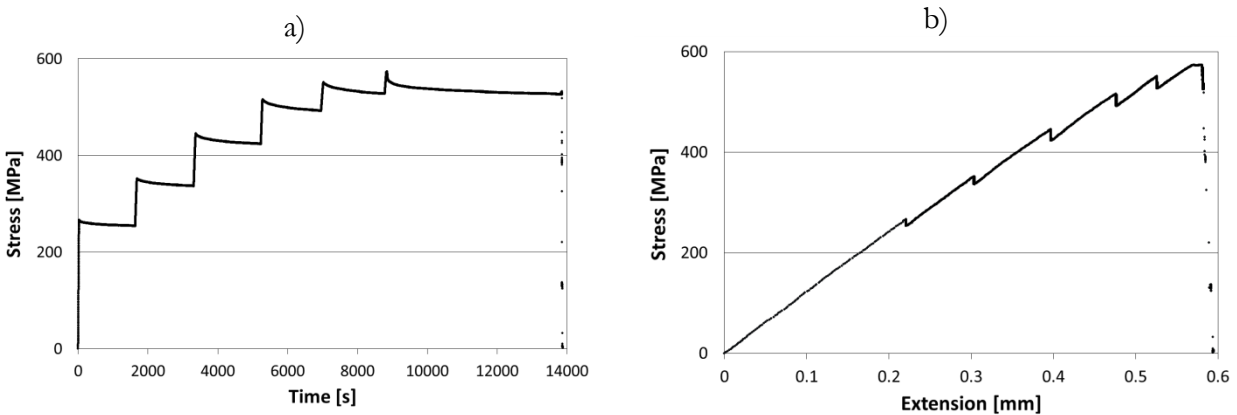
reduced towards the plateau.

Figure 5. Typical a) load-time and b) load-extension graphs of an in-situ SEM tensile test. (Test speeds: 0.5 mm/min up to the first step, 0.1 mm/min up to the fourth step and 0.05 mm/min up to the last step.)

2.6. SEM image acquisition

Multiple images (tiles) covering the central part (~7 mm) of the specimen were recorded at subsequent nearly constant stress levels from zero up to the interlaminar crack propagation stress. The individual images were recorded with 10% overlaps suitable for later stitching of the tiles as shown in Figure 6. Special care has been taken to keep the centre of image no. 1. at the same position for each load step to make the post-processing easier. The SEM images only covered around 65% of the specimen thickness including one full glass layer and the full central carbon layer (see figure 6.). This restriction of the region of interest was necessary in order to optimise the spatial resolution of the images, which were recorded at the full resolution (3072*2304 pixels) of the Zeiss EVO MA15 microscope at moderate (x300) magnification. Figure 3. shows an individual SEM image with 0.3262 μm/pixel resolution saved in an uncompressed file format (8-bit grayscale .tiff) and the level of detail it offers for post-processing. The combination of the highest available resolution and a moderate magnification resulted in the maximum area captured with a high level of detail and the minimum number of stitching zones generated during the post-processing steps.
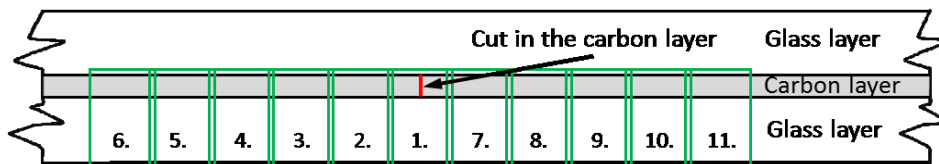

Figure 6. Schematic of the SEM image acquisition scheme on the in-situ tensile test specimen surfaces

2.7. Post-processing of the SEM images

The most important post-processing step on the images taken by the microscope was the stitching of the individual images (tiles) into one single high resolution mosaic image without any loss of quality. This was done in Image J v 2.0. software with a plugin called Mosaic J. The tiles were pre-

aligned manually, and then the built-in algorithm performed the fine adjustment of the overlapping images allowing only for translations (rotation was blocked). The overlapping areas were "blended" by the software to create an even smoother transition between the tiles. It was observed, that the tiles had lower quality (became blurred) towards the corners so these parts of the stitching regions were considered as possible weak spots for image correlation.

After stitching the tiles the mosaic images corresponding to subsequent stress levels were cropped to the same pixel size in the general purpose image processing software Gimp 2 as this is required for image correlation.

2.8. Correlation of the mosaic SEM images

Dantec Dynamic's Istra 4D v 4.3 software was applied for correlating the mosaic images with a spatial resolution of 0.3262 μm/pixel to work out the displacement fields of the tensile specimens. The key parameters of the image correlation, the subset or facet size, (which is the size of the sub-areas the correlation algorithm tracks) and grid spacing (which defines the points where output is generated) were set to 17 pixels (5.55 μm) and 12 pixels (3.91 μm) respectively based on parametric studies to maximise the number of correlated facets and improve the spatial resolution. The optimum facet size was controlled by the particle size and distribution on the specimen surface and the grid spacing was kept as low as possible to ensure the highest possible spatial resolution. As a result a significant overlap was set between the adjacent subsets, which did not compromise the independence of results for each subset [50].

3. Results and discussion

This section presents and explains the results of SEM image acquisition and DIC post-processing. The stresses were calculated based on the original measured full cross-sectional area of the specimen.

3.1. High resolution mosaic images of the delaminating interfaces

Since it is a unique opportunity to observe micrographs of delaminating composite interfaces at subsequent stress levels it worth discussing some of the observations. Figure 7. shows the mosaic image of one half of the scanned area of the specimen at two different stress levels at the early stage of crack propagation. First of all the opening of the initial through thickness cut in the carbon layer and the progress of the visible interlaminar crack tip can be seen. It is also worth noting, that the mode II crack appears to be sharp at a given stress level (Section 1 on Figure 7.), but the newly formed section (Section 2 on Figure 7.) of the same crack shows a completely different appearance (i.e. shear hackles) at the next load step. This interesting behaviour suggests that the properties of an interface may not be identical along the length therefore one single crack may show different appearances along specific sections.
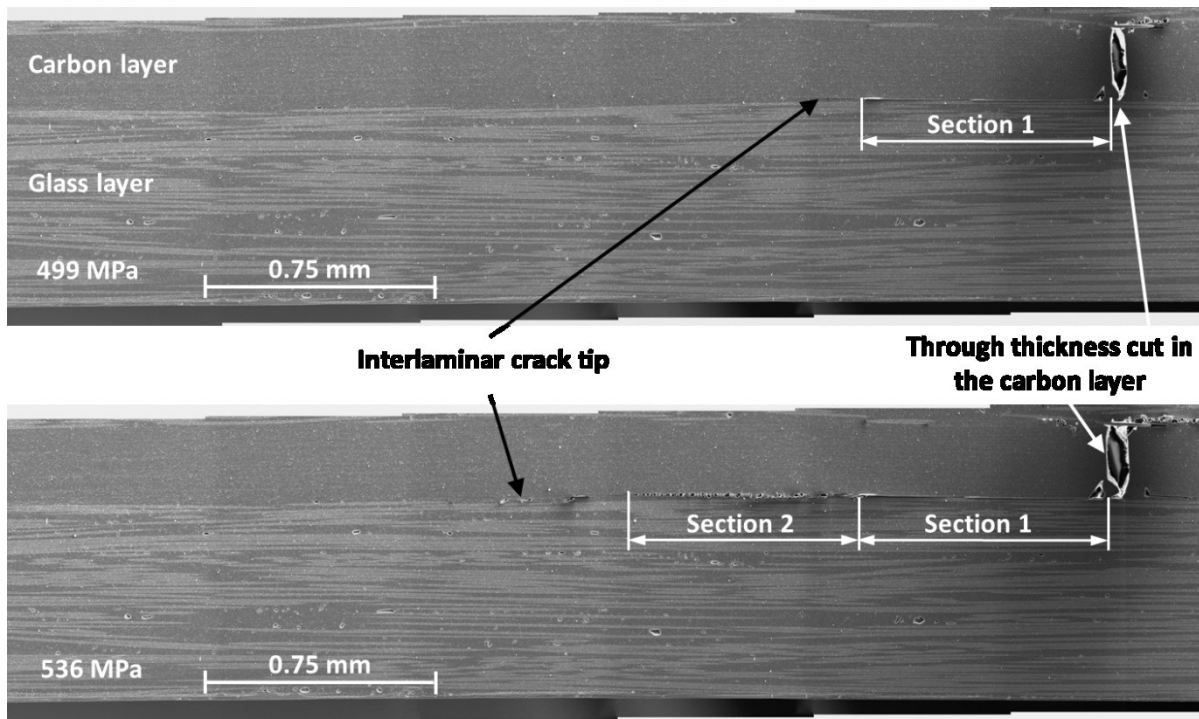

Figure 7. Mosaic images of the delaminating interfaces in a UD glass/carbon hybrid composite at two different tensile stress levels

3.2. Full displacement fields

Figure 8. shows the full displacement fields at three different stress levels obtained by the image correlation of mosaic scanning electron micrographs. The palette used is not suitable for quantitative representation of the data (this is the reason for no colour scale), but very useful to show the overall shape and correlation quality (degree of continuity, missing data etc.) of the displacement fields over a relatively large area (~1x7 mm) of the specimen. The black spots in the correlated fields indicate missing data due to unsuccessful correlation of the corresponding subset. It is obvious that the opening central crack in the carbon layer resulted in a growing uncorrelated patch because the new surfaces were not coated with gold and started to charge, therefore appearing bright (see Figure 7.). The other reason for structured missing data is the stitch areas, which show up especially towards the sides of the displacement fields. Despite a significant amount of missing data, Figure 8. confirms that the image correlation algorithm was robust enough to work around the affected areas and therefore the overall shape, continuity and accuracy of the field were not affected. The highlighted contours make the discontinuities of the displacement field across the damaged interfaces highly visible and visualize the deformed shape of the specimen surface. It is interesting to note that the displacements are not homogeneous within the central carbon ply block. This allows for analysis of the shear stresses in the next phase of the work.
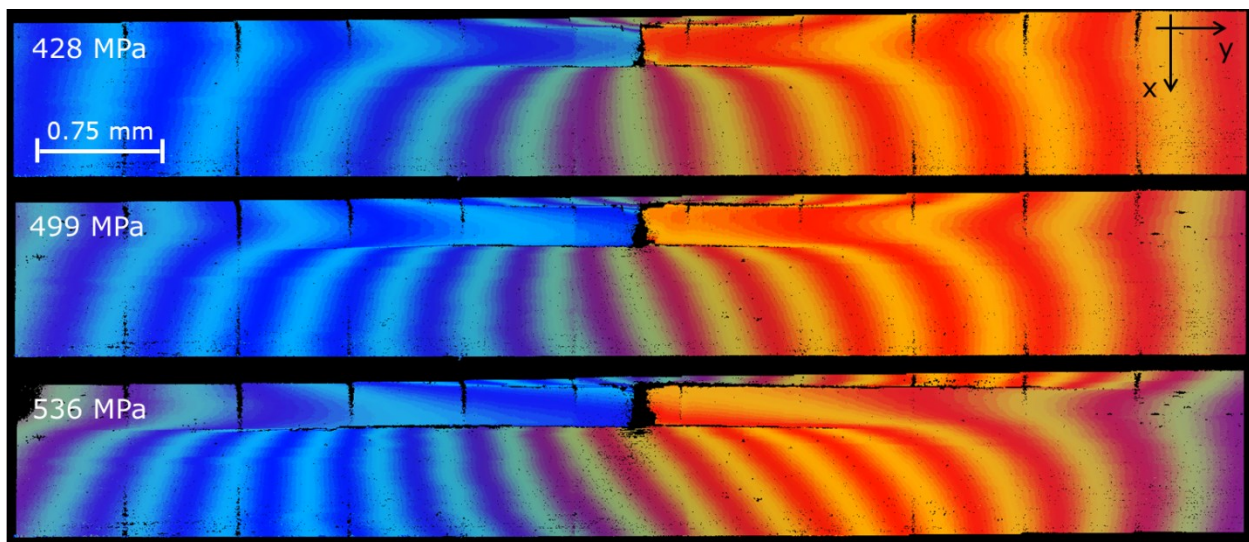
Figure 8. Full y displacement fields of the same UD glass/carbon hybrid composite specimen at various tensile stresses with highlighted displacement contours

The plots of Figure 9. makes quantitative assessment of the deformations of the delaminating layers possible, by comparing colour intensities according to the provided color scale. It is visible on both Figures 8. and 9. that the displacement field is closer to symmetric at the lowest stress level, and becomes more asymmetric at higher stress levels. The reason for this is that any variation of the geometry or material properties of the interfaces can let one of the four mode II cracks propagate a little further than the others, redistributing the loads in the whole specimen. The advantage of the specimen design is, that the analysis of the deformations and stresses can be executed for all four interfaces and suitable compensation techniques (e.g. averaging) can be found to minimise the effect of asymmetry.
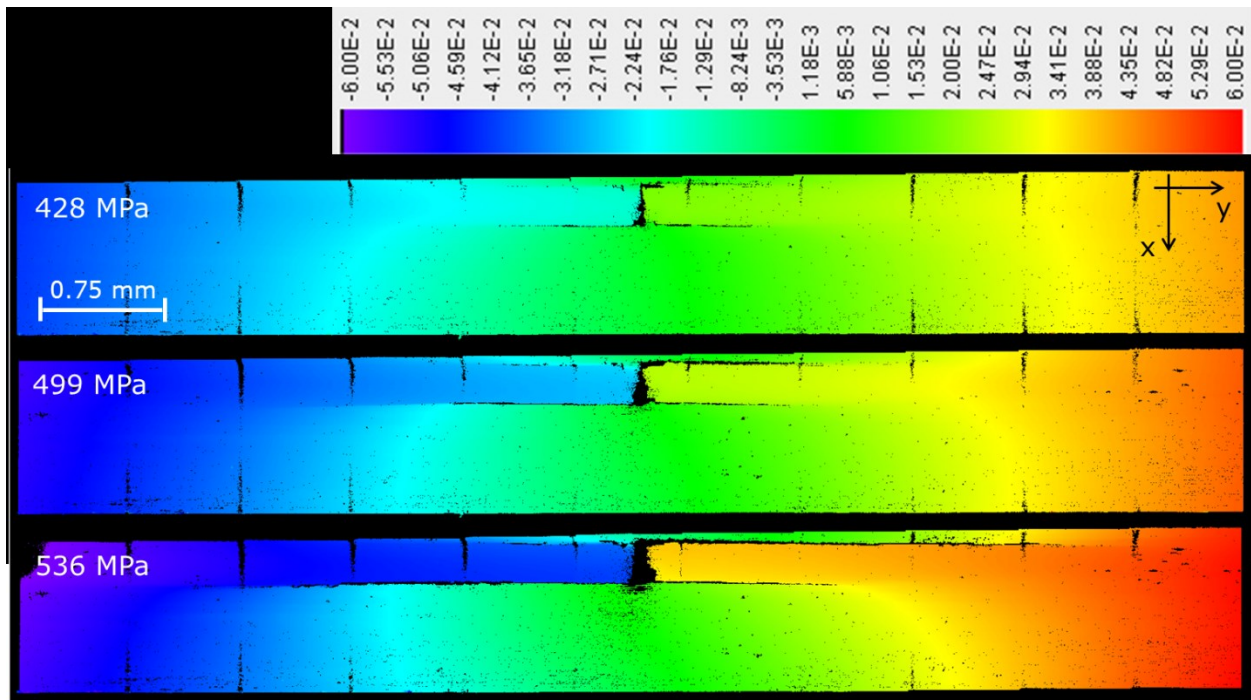

Figure 9. Full y displacement fields of the same UD glass/carbon hybrid composite specimen at various tensile stresses

The full displacement field data is suitable for analysis of the displacement jumps across the interface in the adjacent UD composite layers, which is one of the two required parameters for generating the cohesive law experimentally. Figure 10. shows the displacement plots along lines at various y distances from the initial cut in the carbon layer. The plots show the high quality, low scatter and the sub-micron (less than 0.1 μm) displacement resolution of the full field data which makes it suitable for future quantification of the cohesive law.
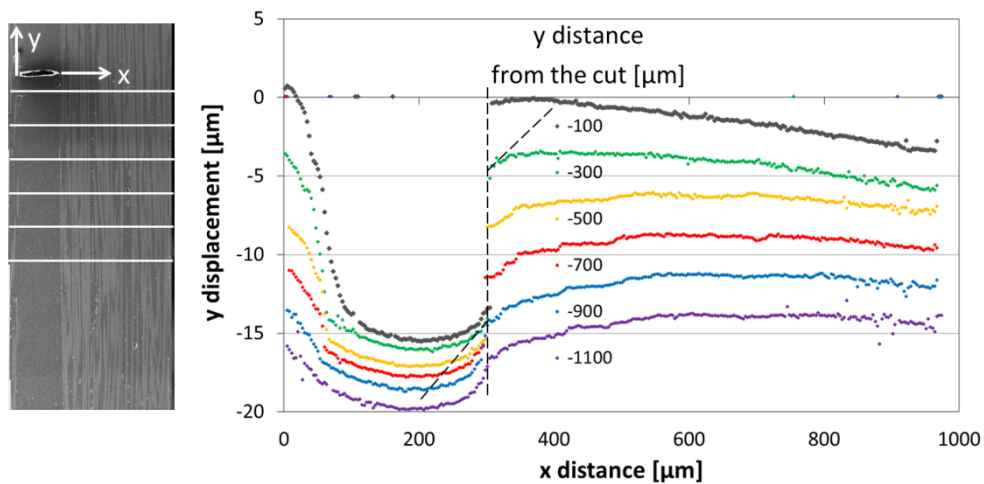

Figure 10. Plots of y displacements across the thickness (x direction) of the hybrid layers at 428 MPa stress level with a schematic showing the positions of the un-deformed lines at various y coordinates

The displacement jumps can be analysed by assigning a straight line for a given interface and recording the y coordinates of its intersections with tangents fitted to the displacement plots from the carbon and glass sides as shown in Figure 10. with dashed lines. The corresponding plot of Figure 10. shows that there is almost zero displacement jump at the interface -1100 μm away from the cut and therefore no more plots were added to the figure. Figure 11. shows example displacement jump plots for the interface analysed on Figure 7. and 10. (lower left). The nearly linear sections of the plots of Figure 11. close to the initial cut in the carbon layer indicate the movement of an unloaded carbon ply block relative to its position before separation from the glass which is

19

loaded at approximately constant strain. This suggests that there is little or no stress transfer through this part of the interface, therefore it can be interpreted as an open interlaminar crack. On the other hand, the asymptotically horizontal ends of the curves indicate that the layers are moving together there, therefore the interface is intact. The non-linear sections between the linear and flat parts indicate the damage process zones. The plots of Figure 11. suggest that the length of the damage process zone for the specific specimen configuration and materials is in the order of 0.5-1 mm.
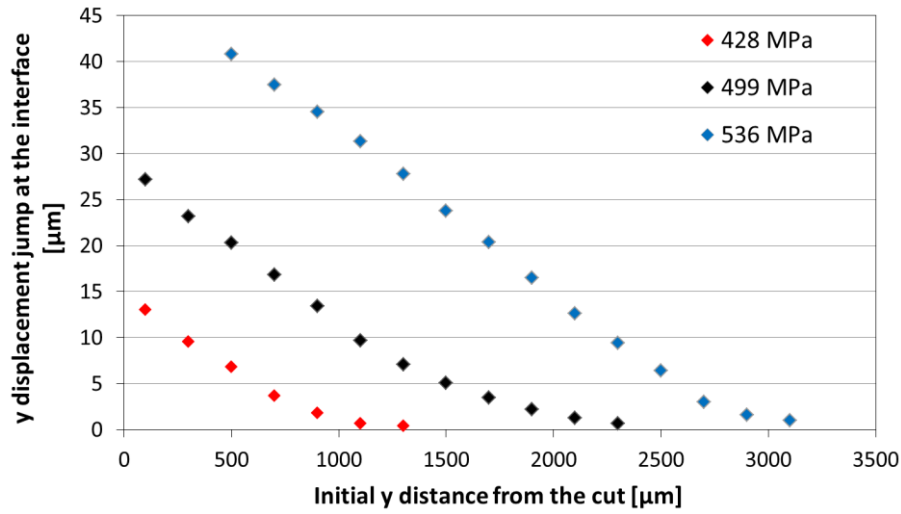

Figure 11. Comparison of displacement jumps at subsequent stress levels in function of the y distance

The calculation of the shear stresses (i.e. traction) is more challenging because it is not as direct as the displacement jump (i.e. separation) assessment and needs suitable numerical procedures, therefore it will be reported in a separate paper.

4. Conclusions

The following conclusions were drawn from the study of delaminating unidirectional carbon/glass fibre reinforced epoxy interlayer hybrid composites:

- A novel stable mode II fracture test setup based on a simple tensile loading scenario was proposed which allows high resolution in-situ SEM image acquisition of delaminating composite layer interfaces. A matching discontinuous interlayer hybrid composite specimen

type was developed which is capable of being tested in tension in-situ in an SEM and shows stable mode II interlaminar crack propagation suitable for imaging at subsequent load steps.

- A suitable surface preparation procedure including submicron alumina particle deposition was found which makes digital image correlation possible on the acquired SEM images.

- An optimised imaging methodology was developed which consists of recording the area of interest with overlapped, high resolution SEM images at moderate magnification and stitching them afterwards into mosaic images. This technique ensures the highest level of detail and maximum covered area with minimum number of stitch lines.

- The deformations of the composite layer interfaces were successfully captured at subsequent stress levels during the in-situ tensile tests in a SEM. The full displacement fields of 1x7 mm areas of the tested specimen were correlated on a 4 μm grid with better than 0.1 μm displacement resolution.

- The generated full displacement fields of composite layer interfaces undergoing damage allowed for unique observations e.g. of the appearance of the mode II cracks, approximate damage process zone length and direct quantitative analysis of the displacement jumps across the interfaces.

- The displacement data can be extensively post-processed and exploited to help understand the mode II interfacial behaviour of composite laminates. Further research is planned to develop suitable procedures for the analysis of the shear stresses at the interfaces which can yield an experimentally determined mode II cohesive law.

5. Acknowledgement

Research grant EP/K004581/1 in collaboration with Madrid Institute for Advanced Studies of

Materials (IMDEA Materials Institute) where the in-situ SEM tensile tests were executed. Gergely

Czél acknowledges the Hungarian Academy of Sciences for funding through the Post-Doctoral

Researcher Programme fellowship scheme. The authors thank Juan Carlos Rubalcaba for his help

with the in-situ SEM measurements.

Supporting data are available, subject to a non-disclosure agreement. Please contact the

corresponding author in the first instance.

6. References

[1] Camanho PP, Davila CG, Pinho ST. Fracture analysis of composite co-cured structural joints using decohesion elements. Fatigue Fract Eng Mater Struct 2003;27:745–57.
[2] Blackman BRK, Hadavinia H, Kinloch AJ, Williams JG. The use of a cohesive zone model to study the fracture of fibre composites and adhesively-bonded joints. Int J Fract 2003;119:25–46.
[3] Li S, Thouless MD, Waas AM, Schroeder JA, Zavattieri PD. Mixed-mode cohesive-zone models for fracture of an adhesively bonded polymer–matrix composite. Eng Fract Mech 2006;73:64–78.
[4] Goyal VK, Johnson ER, Goyal VK. Predictive strength-fracture model for composite bonded joints. Compos Struct 2008;82:434–46.
[5] Wisnom MR. Modelling discrete failures in composites with interface elements. Composites Part A 2010;41:795–805.
[6] Mi Y, Crisfield MA, Davies GAO, Hellweg H-B. Progressive delamination using interface elements. J Compos Mater 1998;32:1246–72.
[7] Petrossian Z, Wisnom MR. Prediction of delamination initiation and growth from discontinuous plies using interface elements. Compos A: Appl Sci Manufactur 1998;29A:503–15.
[8] Chen J, Crisfield M, Kinloch AJ, Busso EP, Matthews FL, Qiu Y. Predicting progressive delamination of composite material specimens via interface elements. Mech Compos Mater Struct 1999;6:301–17.
[9] Crisfield MA, Alfano G. Finite element interface models for the delamination analysis of laminated composites: mechanical and computational issues. Int J Num Meth Eng 2000;50:1701–36.
[10] Camanho PP, Davila CG, De Moura MF. Numerical simulation of mixed-mode progressive delamination in composite materials. J Compos Mater 2003;37:1415–24.
[11] Yang Q, Cox B, Cohesive models for damage evolution in laminated composites. Int J Fract 2005;133:107–37.
[12] Pinho ST, Ianucci L, Robinson P. Formulation and implementation of decohesion elements in an explicit finite element code. Compos A: Appl Sci Manufactur 2006;37:778–89.

[13] Jiang WG, Hallett SR, Green BG, Wisnom MR. A concise interface constitutive law for analysis of delamination and splitting in composite materials and its application to scaled notched tensile specimens. Int J Num Meth Eng 2007;69:1982–95.

[14] Turon A, Davila CG, Camanho PP, Costa J. An engineering solution for mesh size effects in the simulation of delamination using cohesive zone models. Eng Fract Mech 2007;74:1665–82.

[15] Turon A, Costa J, Camanho PP, Davila CG. Simulation of delamination in composites under high-cycle fatigue. Compos A: Appl Sci Manufactur 2007;38:2270–82.

[16] Harper PW, Hallett SR. Cohesive zone length in numerical simulations of composite delamination. Engineering Fracture Mechanics, 2008;75:4774-4792.

[17] Jalalvand M, Wisnom MR, Hosseini-Toudeshky H, Mohammadi B. Experimental and numerical study of oblique transverse cracking in cross-ply laminates under tension. Composites Part A, 2014;67:140-148.

[18] Jalalvand M, Czél G, Wisnom MR. Numerical modelling of the damage modes in UD thin carbon/glass hybrid laminates. Compos Sci Technol 2014;94:39–47.

[19] Elices M, Guinea GV, Gómez J, Planas J. The cohesive zone model advantages, limitations and challenge. Eng Fract Mech 2002;69:137–63.

[20] Cornec A, Scheider I, Schwalbe KH. On the practical application of the cohesive model. Eng Fract Mech 2003;70:1963–87.

[21] de Borst R. Numerical aspects of cohesive-zone models. Eng Fract Mech 2003;70:1743–57.

[22] Xie D, Waas AM. Discrete cohesive zone model for mixed-mode fracture using finite element analysis. Eng Fract Mech 2006;73:1783–96.

[23] Brewer JC, Lagace PA. Quadratic Stress Criterion for Initiation of Delamination. J Compos Mater 1988;22:1141–55.

[24] O'Brien T. Characterization of delamination onset and growth in a composite laminate. in Damage in Composite Materials. Editor: K. Reifsnider, ASTM STP 1982:140–67.

[25] Corigliano A. Formulation, identification and use of interface models in the numerical analysis of composite delamination. Int J Solids Struct 1993;30:2779–811.

[26] Van den Bosch MJ, Schreurs PJG, Geers MGD. An improved description of the exponential Xu and Needleman cohesive zone law for mixed-mode decohesion. Eng Fract Mech 2006;73:1220–34.

[27] Tvergaard V, Hutchinson JW. The relation between crack growth resistance and fracture process parameters in elastic-plastic solids. J Mech Phys Solids 1992;40:1377–97.

[28] Balzani C, Wagner W. An interface element for the simulation of delamination in unidirectional fiber-reinforced composite laminates. Eng Fract Mech 2008;75:2597–615.

[29] Wisnom MR. Modelling of stable and unstable fracture of short beam shear specimens. Composites 1994;25:394–400.

[30] Shet C, Chandra N. Effect of the shape of traction–displacement cohesive zone curves on the fracture response. Mech Adv Mater Struct 2004;11:249–75.

[31] Sills RB, Thouless MD. The effect of cohesive-law parameters on mixed-mode fracture. Engineering Fracture Mechanics, 2013;109:353-368.

[32] Sørensen BF, Kirkegaard P. Determination of mixed mode cohesive laws. Eng Fract Mech 2006;73:2642–61.

[33] Sørensen BF, Jacobsen TK. Characterizing delamination of fibre composites by mixed mode cohesive laws. Compos Sci Technol 2009;69:445–56.

[34] De Moura MFSF, Gonçalves JPM, Magalhães AG. A straightforward method to obtain the cohesive laws of bonded joints under mode I loading. Int J Adhes Adhes 2012;39:54–9.

[35] Fernandes RMRP, Chousal JAG, de Moura MFSF, Xavier J. Determination of cohesive laws of composite bonded joints under mode II loading. Composites Part B: Engineering. 3013;52:269-274.

[36] Dourado N, de Moura MFSF, de Morais AB, Pereira AB. Bilinear approximations to the mode II delamination cohesive law using an inverse method. Mechanics of Materials, 2012;49:42-50.

[37] Cui H, Koussios S, Li Y, Beukers A. Constitutive law of adhesive layer measured with mixed mode bending test. Engineering Fracture Mechanics 2014;127: 235–251.

[38] González C, LLorca J. Mechanical behavior of unidirectional fiber-reinforced polymers under transverse compression: microscopic mechanisms and modeling. Compos Sci Technol 2007;67:2795–806.

[39] Canal LP, González C, Segurado J, LLorca J. Intraply fracture of fiber-reinforced composites: Microscopic mechanisms and modelling. Composites Science and Technology. 2012;72:1223–1232.

[40] Canal LP, González C, Molina-Aldareguía JM, Segurado J, LLorca J. Application of digital image correlation at the microscale in fiber-reinforced composites Composites Part A: Applied Science and Manufacturing, 2012;43:1630-1638.

[41] Mortell DJ. Tanner DA. McCarthy CT. In-situ SEM study of transverse cracking and delamination in laminated composite materials. Composites Science and Technology. 2014;105:118–126.

[42] Cui W, Wisnom MR, Jones MI. An experimental and analytical study of delamination of unidirectional specimens with cut central plies. J Reinf Plast Compos 1994;13:722-739.

[43] Jalalvand M, Czél G, Wisnom M. Damage analysis of pseudo-ductile thin-ply UD hybrid composites – A new analytical method. Composites Part A: Applied Science and Manufacturing 2015;69:83-93.

[44] Czél G, Jalalvand M, Wisnom MR. Development of pseudo-ductile hybrid composites with discontinuous carbon- and continuous glass prepregs. 2014. Paper presented at ECCM 16, Seville, Spain.

[45] Czél G, Wisnom MR. Demonstration of pseudo-ductility in high performance glass-epoxy composites by hybridisation with thin-ply carbon prepreg. Compos Part A Appl Sci Manuf 2013;52:23–30.

[46] Czél G, Jalalvand M, Wisnom MR. Demonstration of pseudo-ductility in unidirectional hybrid composites made of discontinuous carbon/epoxy and continuous glass/epoxy plies. Composites Part A: Applied Science and Manufacturing. 2015;72:75-84.

[47] Fuller J., Wisnom M. R.: Damage suppression in thin ply angle-ply carbon/epoxy laminates. The 19th International Conference on Composite Materials, Montreal: 2013.

[48] Wisnom M. R., Atkinson J. W.: Reduction in tensile and flexural strength of unidirectional glass fibre-epoxy with increasing specimen size. Compos Struct 1997;38:405-411.

[49] Wisnom MR, Jones MI. Size Effects in Interlaminar Tensile and Shear Strength of Unidirectional Glass Fibre-Epoxy. J Reinf Plast Compos 1996;15:2-15.

[50] Sutton MA, Orteu JJ, Schreier H. Image Correlation for Shape, Motion and Deformation Measurements: Basic Concepts, Theory and Applications. Springer, New York, 2009.